FMS-Like Tyrosine Kinase 3–Internal Tandem Duplication Tyrosine Kinase Inhibitors Display a Nonoverlapping Profile of Resistance Mutations *In vitro*

Nikolas von Bubnoff,[1] Richard A. Engh,[2] Espen Åberg,[2] Jana Sänger,[1] Christian Peschel,[1] and Justus Duyster[1]

[1]III. Medizinische Klinik, Klinikum rechts der Isar, Technische Universität München, München, Germany and [2]The Norwegian Structural Biology Centre, Departments of Chemistry and Pharmacy, University of Tromsø, Tromsø, Norway

Abstract

FMS-like tyrosine kinase 3 (FLT3) inhibitors have shown activity in the treatment of acute myelogenous leukemia (AML). Secondary mutations in target kinases can cause clinical resistance to therapeutic kinase inhibition. We have previously shown that sensitivity toward tyrosine kinase inhibitors varies between different activating FLT3 mutations. We therefore intended to determine whether different FLT3 inhibitors would produce distinct profiles of secondary, FLT3 resistance mutations. Using a cell-based screening approach, we generated FLT3–internal tandem duplication (ITD)–expressing cell lines resistant to the FLT3 inhibitors SU5614, PKC412, and sorafenib. Interestingly, the profile of resistance mutations emerging with SU5614 was limited to exchanges in the second part of the kinase domain (TK2) with exchanges of D835 predominating. In contrast, PKC412 exclusively produced mutations within tyrosine kinase domain 1 (TK1) at position N676. A mutation at N676 recently has been reported in a case of PKC412-resistant AML. TK1 mutations exhibited a differential response to SU5614, sorafenib, and sunitinib but strongly impaired response to PKC412. TK2 exchanges identified with SU5614 were sensitive to PKC412, sunitinib, or sorafenib, with the exception of Y842D, which caused a strong resistance to sorafenib. Of note, sorafenib also produced a highly distinct profile of resistance mutations with no overlap to SU5614 or PKC412, including F691L in TK1 and exchanges at position Y842 of TK2. Thus, different FLT3 kinase inhibitors generate distinct, nonoverlapping resistance profiles. This is in contrast to Bcr-Abl kinase inhibitors such as imatinib, nilotinib, and dasatinib, which display overlapping resistance profiles. Therefore, combinations of FLT3 inhibitors may be useful to prevent FLT3 resistance mutations in the setting of FLT3-ITD–positive AML. [Cancer Res 2009;69(7):3032–41]

Introduction

The type III receptor tyrosine kinase FMS-like tyrosine kinase 3 (FLT3) constitutes a potentially attractive therapeutic target in acute myelogenous leukemia (AML). FLT3 is overexpressed in most patients with AML (1). In addition, activating FLT3 mutations can be identified in approximately one-third of AML patients. Internal tandem duplication (ITD) mutations within the juxtamembrane domain are most common, whereas single-base point mutations, small deletions, or insertions within the receptor tyrosine kinase domain activation loop (FLT3-TKD) constitute the minority of cases (2, 3). Both classes of mutations lead to constitutive activation of the receptor and downstream signaling events in the absence of ligand (4), and FLT3-ITDs induce a lethal myeloproliferative disease in murine bone marrow transplantation experiments (5). Small molecule inhibitors of FLT3 tyrosine kinase such as PKC412 or CEP701 were shown to be effective in preclinical models (6, 7) and showed activity in clinical trials (8, 9). However, the majority of patients display primary or secondary resistance to FLT3 inhibitors (8, 9), and a case of a patient with a FLT3-ITD resistance mutation and AML resistant to PKC412 already has been described (10). At this time, a growing number of FLT3 inhibitors enter preclinical and clinical evaluation (11). For the indolinone SU11248 (Sunitinib, Sutent), phase I data indicate clinical activity in FLT3-mutated AML (12), and the biaryl urea BAY 43-9006 (Sorafenib, Nexavar) displayed promising FLT3 activity *in vitro* (13, 14), and recently entered clinical evaluation in FLT3 wild-type (wt) and mutant AML (15). We have shown before that sensitivity toward specific FLT3 kinase inhibitors varies between different activating FLT3 mutations (14, 16). Therefore, we intended to determine whether different FLT3 inhibitors on a FLT3-ITD background would be prone to similar secondary mutations that might cause clinical resistance to FLT3 inhibitors. Using an *in vitro* resistance screening approach (17), we here show that the resulting profiles of resistance mutations were largely nonoverlapping. This *in vitro* data indicate that combinations of FLT3 inhibitors may be beneficial to prevent resistance due to FLT3-ITD kinase domain mutations in AML.

Materials and Methods

Inhibitors. PKC412 was a kind gift from Novartis Pharma AG. SU5614 was obtained from Calbiochem-Novabiochem. Sorafenib was purchased from American Chemicals Custom Corporation. Sunitinib was purchased from a local pharmacy. Each compound was dissolved in DMSO to give a 10 mmol/L stock solution and stored at −20°C. Chemical structures of the compounds are shown in Supplementary Fig. 1.

Cell culture and DNA constructs. Ba/F3 cell lines expressing FLT3-ITD constructs were established and maintained as described previously (14). FLT3-ITD cDNA was kindly provided by Hubert Serve (4). Point mutations were engineered in Mig EGFP FLT3-ITD using the QuickChange mutagenesis kit (Stratagene). All constructs were verified using automated sequencing. Total RNA was extracted with TRIzol reagent (Invitrogen). For reverse-transcription PCR of a 1652-bp fragment of FLT3 encompassing transmembrane domain, juxtamembrane domain, and kinase domain, the primers used were as follows: 5′-GTCCTGTTCCTCTGATGGCTACCCCCTAC-3′ and

Requests for reprints: Nikolas von Bubnoff, III. Medizinische Klinik, Klinikum rechts der Isar, Technische Universität München, Ismaningerstraβe 22, 81675 München, Germany. Phone: 49-89-41405835; Fax: 49-89-41404879; E-mail: n.bubnoff@lrz.tum.de.

doi:10.1158/0008-5472.CAN-08-2923

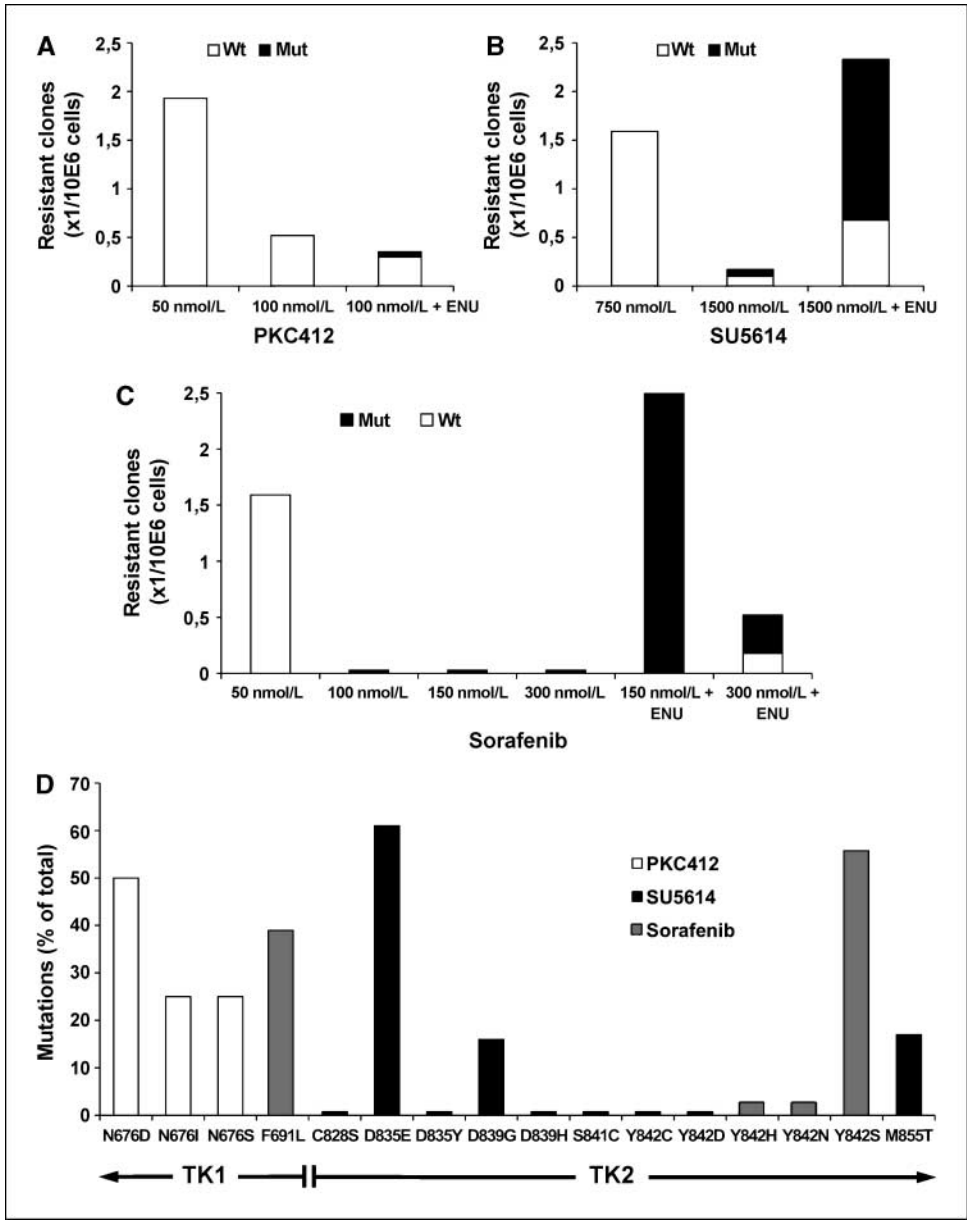

Figure 1. Frequency of resistant clones in the PKC412 (*A*), SU5614 (*B*), and sorafenib screen (*C*) and distribution of identified exchanges in FLT3 (*D*). Ba/F3 Mig EGFP FLT3-ITD wt cells were cultured in 96-well plates in the presence of inhibitor at the indicated concentrations. Resistant colonies were picked and analyzed for the presence of point mutations within the FLT3-ITD kinase domain. Wild-type (*open bars*) and mutant (*filled bars*) clones are shown separately. The frequency is shown as resistant clones per million cells at the beginning of culture (*A–C*). The position and relative abundance of different mutations is depicted for PKC412 (*open bars*), SU5614 (*black bars*), and sorafenib (*gray bars*). PKC412 resistance mutations occurred in FLT3-ITD TK1, SU5614 mutations were limited to TK2, and sorafenib mutations came up at distinct sites in TK1 and TK2 (*D*). Three exchanges at TK1 N676 were identified with PKC412, nine exchanges affecting six different positions in TK2 were identified in cell clones resistant to SU5614, and exchanges emerging with sorafenib included F691L in TK1 and three different exchanges at Y842 in TK2.

5′-CTGTGAATCTTCACCTGGGCCTGTGGCGATG-3′. Using this fragment as template, the following primers were used for nested PCR and sequence analysis: for juxtamembrane domain including ITD, tyrosine kinase domain 1 (TK1) and joining domain: 5′-GCAACAATTGGTGTTT-GTCTCCTC-3′ and 5′-GGTCTCTGTGGACACACGACTTGAAC-3′; and for tyrosine kinase domain 2 (TK2): 5′-CAGTTACACCCGCCCTTGGATCAG-3′ and 5′-GGATGGATGTTCTGGGACGTTGC CAC-3′.

Resistance screen. Screening for inhibitor-resistant colonies was performed as described previously (17). When indicated, Ba/F3 Mig EGFP/FLT3-ITD cells were pretreated twice with N-ethyl-N-nitrosourea (ENU) for 8 h at a concentration of 100 μg/mL. Thereafter, cells were cultured in 96-well plates at a density of 4×10^5 per well in the presence of PKC412 at 50 or 100 nmol/L, SU5614 at 750 or 1,500 nmol/L, and sorafenib at 50, 100, 150, or 300 nmol/L. Culture supernatants were replaced by fresh medium containing inhibitor after 48 h. Cell colonies that became visible were picked, expanded, and analyzed. Resulting inhibitor-resistant sublines were cultured in the presence of inhibitor at a concentration corresponding to that used during the screen, except for sublines emerging in the presence of PKC412 at 100 nmol/L, which were maintained in the presence of PKC412 at 50 nmol/L.

Proliferation. Cell proliferation was measured using an 3-(4,5-dimethylthiazol-2-yl)-5-[3-carboxymethoxyphenyl-2-(4-sulfophenyl)-2H-tetrazolium (MTS)]-based method by absorption of formazan at 490 nm (CellTiter 96; Promega). Measures were taken in triplicates after 24 and 48 h of culture.

Western blot. Ba/F3 cells were cultured for 2.5 h without and in the presence of inhibitor at the indicated concentrations. Cell lysis, SDS-PAGE, and immunoblotting were done as described previously (17). Antibodies to phospho-FLT3 (Tyr589/591) were obtained from Cell Signaling (clone 30D4; New England Biolabs GmbH). FLT3 antibodies were purchased from Upstate Biotechnology (#06-647; Millipore). Bands were visualized using the enhanced chemoluminescence system (Amersham).

Structural modeling. The protein crystal structures[3] were superimposed with alignment of α carbon positions with PyMOL[4] using 1RJB (18) as reference coordinate set. Inspections were performed and structure figures were created with PyMOL.

[3] http://www.pdb.org
[4] http://pymol.sourceforge.net/

Results

Screening for FLT3 TKI-resistant Ba/F3 clones reveals distinct mutation profiles for SU5614 and PKC412. To generate FLT3 tyrosine kinase inhibitor–resistant cell lines, we cultured Ba/F3 FLT3-ITD cells in 96-well plates in the presence of the FLT3 inhibitors PKC412, SU5614, or sorafenib. For the staurosporine derivative PKC412, we used 50 and 100 nmol/L, corresponding to 6.25 and 12.5 times the cellular IC_{50} value in Ba/F3 FLT3-ITD cells. At 50 nmol/L PKC412, 74 of 96 wells displayed growth, whereas at 100 nmol/L, only 20 of 96 wells were growing, corresponding to a clone frequency of 1.93 and 0.52 per million cells input, respectively (Fig. 1*A*). However, when we sequenced the entire FLT3-ITD kinase domain for mutations that might have caused outgrowth of PKC-resistant subclones, we were not able to detect point mutations in any of these clones. We therefore pretreated Ba/F3 FLT3-ITD cells with the mutagene ENU (19). Using these cells, we obtained 27 clones, and 4 of these displayed mutations (Fig. 1*A*). In all cases, the resulting amino acid exchanges affected position N676 within the first part of the FLT3 kinase domain (TK1), two clones with an exchange to aspartic acid, one to isoleucine, and one to serine, respectively (Fig. 1*D*). In accordance, an exchange at N676 to Lysine has been described in a case of PKC412 resistant, FLT3-ITD–positive AML (10). Of note, no mutations in TK2 were identified in PKC412-resistant cell clones. We next intended to determine whether a structurally different FLT3 inhibitor, the indolinone derivative SU5614 would produce a similar or distinct profile of resistance mutations. To this end, we cultured Ba/F3 FLT3-ITD cells in the presence of SU5614 at 750 and 1500 nmol/L, corresponding to 7.5 and 15 times the cellular IC_{50} value. Similar to PKC412, low concentrations of the drug gave rise to a high number of resistant clones with growth in 61 of 96 wells, corresponding to a clone frequency of 1.59 per million cells input (Fig. 1*B*). The yield of resistant clones decreased to 13 wells with growth of 192 at 1,500 nmol/L, corresponding to 0.17 clones per million cells. Pretreatment with ENU resulted in a substantial increase of resistant clones: 179 of 192 wells displayed outgrowth, the appendant clone frequency was as high as 2.33 compared with 0.17 without ENU pretreatment (Fig. 1*B*). Examination of FLT-ITD for mutations giving rise to SU5614 resistance exclusively revealed exchanges in TK2, and in contrast to PKC412, no TK1 exchanges were identified. Although none of the 61 clones derived from the SU5614 screen with 750 nmol/L contained mutations, 5 of 8 clones at 1,500 nmol/L (without ENU) harbored 4 different exchanges at positions S841, Y842, and D839 within the FLT3 activation loop, respectively (Fig. 1*C*). Remarkably, in clones that emerged at 1,500 nmol/L SU5614 after ENU treatment, 127 of 179 clones (71%) displayed mutations, generating 9 different exchanges affecting 6 positions in the activation loop. Exchanges of D835, in all but one cell clone to glutamic acid predominated (65%), followed by M855T (18%; Fig. 1*D*). Together, all exchanges that came up in the presence of SU5614 comprised the narrow region from C828 to M855 in the activation loop, whereas PKC412 exclusively produced exchanges of position N676. Thus, these FLT3 inhibitors generated distinct, nonoverlapping profiles of resistance mutations.

PKC412 and SU5614 display limited cross-resistance. We went on to explore whether the marked difference in the resistance profiles generated with PKC412 and SU5614 would be reflected by a lack of cross resistance between both compounds with regard to the exchanges that were detected in the respective screens. We therefore cloned all identified FLT3-ITD mutations, generated stable cell lines, and examined FLT3-ITD autophosphorylation and cell growth in the presence of PKC412 and SU5614. TK1 exchanges that emerged in the PKC412 screen induced an increase of cellular IC_{50} values in the presence of PKC412 in the range of factor 3.1 (N676S) to factor 10 (N676D; Supplementary Fig. S2*A, top*; see Table 1). This was accompanied by retained FLT3-ITD autophosphorylation in the presence of PKC412 (Fig. 2*A*). Two of three N676 exchanges identified in the presence of PKC412 also gave rise to a significant SU5614 resistance (Supplementary Fig. S2*A, bottom*; Table 1). Although the N676S exchange did not alter SU5614 response, the exchanges to isoleucine and aspartic acid shifted IC_{50} values by a factor of 4 compared with FLT3-ITD wt cells. All TK2 exchanges identified in SU5614-resistant clones shifted cellular SU5614 response by factor 1.25 (S841C) to factor 5 (D835Y, Y842C; see Supplementary Fig. S2*B, top* and Table 1). Again, protection from growth suppression correlated well with persistent FLT3-ITD autophosphorylation in the presence of SU5614 (Fig. 2*B*), confirming that the identified TK2 exchanges caused inhibitor resistance. Interestingly, TK2 exchanges identified in the SU5614 screen only marginally interfered with response to PKC412 (Supplementary Fig. S2*B, bottom*; Table 1). Cellular IC_{50} values shifted at maximum by a factor of 2.5 (D839G, M855T), whereas other exchanges corresponded to FLT3-ITD wt (S841C, Y842N), or were even more sensitive as wt cells (Y842C, Y842D, Y842H, Y842S).

Thus, although two of three PKC412 TK1 exchanges also were resistant to SU5614, SU5614 TK2 mutations did not cause significant cross-resistance to PKC412.

SU11248 and sorafenib are active against PKC412 and SU5614-resistant FLT3-ITD mutations. Because the 3-substituted indolinone SU5614 may not enter further clinical testing, we sought to determine whether the structurally similar 3-substituted indolinone SU11248 (sunitinib) would be active against the identified PKC412 and SU5614 FLT3-ITD resistance mutants. Compared with SU5614, SU11248 displayed a significantly higher activity against all SU5614-resistant TK2 mutations (Supplementary Fig. S2*C, top*; Table 1). In contrast, TK1 N676 exchanges identified in the PKC412 screen also caused some decrease in sensitivity for SU11428 (Supplementary Fig. S2*C, bottom*; Table 1). However, complete growth inhibition was observed at 500 nmol/L. We next examined the biaryl urea sorafenib, a structurally distinct FLT3 inhibitor that recently entered clinical evaluation in FLT3 wt and mutant AML. Interestingly, TK2 exchanges responded to sorafenib with the exception of FLT3-ITD Y842D, which in contrast to Y842C or neighboring exchanges in TK2 markedly shifted response to sorafenib by a factor of 31 (Supplementary Fig. S2*D, top;* Table 1). Also, the D839H exchange but not D839G affected sorafenib response. Similar to SU11248, lower absolute inhibitory concentrations were necessary for complete growth suppression of N676 exchanges with sorafenib (125–500 nmol/L; see Supplementary Fig. S2*D, bottom*) compared with SU5614 (500–2,000 nmol/L; Supplementary Fig. S2*A, bottom*).

Screening for sorafenib resistance reveals specific exchanges at FLT3-ITD Y842 and F691. The finding that Y842D but not Y842C or other TK2 exchanges caused a strong resistance to sorafenib prompted us to search for sorafenib-specific resistance mutations in FLT3-ITD. We therefore generated sorafenib-resistant Ba/F3 FLT3-ITD sublines (Fig. 1*C*). With sorafenib at 100 and 150 nmol/L, corresponding to ~13 and 19 times IC_{50} in FLT-ITD wt cells, we discovered two exchanges at Y842 in TK2 (Y842H/N) that did not match the exchanges previously identified with SU5614 at the same site (Y842C/D; see Fig. 1*D*). However, when we

Table 1. Individual mutation patterns for different FLT3 inhibitors in correlation to cellular resistance profiles

Cellular IC_{50} (nmol/L/fold wt)

Wt	PKC412	SU5614	SU11248	Sorafenib
	8/–	100/–	25/–	8/–
TK1				
N676D	80/10	400/4	200/8	100/12.5
N676I	40/5	400/4	100/4	40/5
N676S	25/3.1	100/1	60/2.4	10/1.25
F691I	140/17.5	>2,000/>20	450/18	>1,000/>125
F691L	10/1.25	300/3	90/3.6	>1,000/>125
TK2				
C828S	17.5/2.2	300/3	75/3	9/1.1
D835E	10/1.25	350/3.5	100/4	9/1.1
D835Y	15/1.9	500/5	100/4	9/1.1
D839G	20/2.5	350/3.5	75/3	10/1.25
D839H	10/1.25	300/3	75/3	80/10
S841C	8/1	125/1.25	20/0.8	10/1.25
Y842C	4/0.5	500/5	25/1	10/1.25
Y842D	2/0.25	300/3	50/2	250/31.3
Y842H	4/0.5	700/7	90/3.6	300/37.5
Y842N	9/1.1	1,000/10	225/9	600/75
Y842S	4/0.5	1,000/10	100/4	400/50
M855T	20/2.5	325/3.25	75/3	10/1.25

NOTE: Red, strong resistance; yellow, moderate resistance; green: no/weak, resistance. Exchanges identified in PKC412-, SU5614-, and sorafenib-resistant sublines are indicated by bold frames. Mutations identified in the screens and FLT3-ITD F691I (21) were recreated in FLT3-ITD using site-directed mutagenesis and expressed in Ba/F3 cells. After incubation for 24 and 48 h without and in the presence of SU5614, PKC412, SU11248, or sorafenib at the indicated concentrations, proliferation was measured using an MTS-based method. At least two independent experiments were performed for each FLT3-ITD construct. Representative results of one experiment per inhibitor and construct after 48 h of incubation are expressed as individual cellular IC_{50} values and fold change IC_{50} of FLT3 wt–expressing Ba/F3 cells. Individual dose response is shown in detail in Supplementary Fig. 2. The extent of cellular resistance is indicated as strong (*red*), yellow (*moderate*), and no/weak (*green*) with a cellular IC_{50} range for weak/moderate/strong of <12.5/12.5 to 24.9/≥25 nmol/L for PKC412, and <250/250 to 499/≥500 nmol/L for SU5614, SU11248, and sorafenib.

increased the concentration to 38 times IC_{50} (300 nmol/L), we exclusively isolated F691L in TK1. To increase the yield of mutant clones, we pretreated cells with ENU and again screened with sorafenib at 150 and 500 nmol/L (Fig. 1*C*). At 150 nmol/L, all clones contained FLT3-ITD Y842S, whereas at 300 nmol/L, all cell clones harbored FLT3-ITD F691L. Thus, sorafenib displays a resistance profile in FLT3-ITD distinct from PKC412 and SU5614 and unlike these compounds, the emerging exchanges shift between two distinct sites in TK1 and TK2, depending on the inhibitor concentration. As expected, FLT3-ITD Y842H/N/S and F691L profoundly attenuated cellular and biochemical response to sorafenib 37.5- to >125-fold when cloned and expressed in Ba/F3 cells (Supplementary Fig. S2*E, top*; Table 1; Fig. 2*C*). Response to SU5614 and SU11248 was also affected by these exchanges, although both indolinone type inhibitors fully suppressed the highly sorafenib-resistant F691L exchange at concentrations of 1,000 nmol/L (SU5614; Supplementary Fig. S2*E, bottom*) and 250 nmol/L (SU11248; Supplementary Fig. S2*F, top*). In addition, SU11248 displayed significant activity against the highly sorafenib-resistant Y842 exchanges, with complete growth inhibition at 500 nmol/L (Supplementary Fig. S2*F, top*). In marked contrast, sorafenib resistance mutations did not affect PKC412 response (Supplementary Fig. S2*F, bottom*; Table 1). Of interest, this was also the case for F691L. Position F691 in FLT3-ITD corresponds to T315 in ABL (20), where an exchange to isoleucine causes a full and complete resistance to imatinib, nilotinib, and dasatinib. An exchange at F691 to isoleucine was previously identified by *in vitro* mutagenesis of FLT3-ITD TK1 to cause PKC412 resistance (21). In accord, F691I lead to a 18-fold mitigation of PKC412 drug response (Supplementary Fig. S2*F, bottom*; Table 1; Fig. 2*A*), and strongly affected response to sorafenib and SU5614 (Supplementary Fig. S2*E*). Using SU11248 at 2,000 nmol/L resulted in nearly complete suppression of F691I (Supplementary Fig. S2*F, top*). Together, sorafenib screening identified a set of strong resistance mutations in FLT3-ITD. Most of these exhibited partial cross-resistance to SU5614 and SU11248 but were responsive to PKC412. FLT3-ITD F691I was highly resistant to all compounds, although complete growth inhibition was seen with high concentrations of SU11248.

Structural analysis. Most positions in FLT3-ITD where we identified exchanges in our inhibitor-resistant cell clones correspond to substitutions in related kinases linked to clinical imatinib resistance, supporting the validity of our results (Supplementary Table S1). The inhibitors generated distinct and nearly mutually exclusive sets of resistance mutants (Table 1; Fig. 3). Moreover, the resistance patterns, while overlapping, are unique for each inhibitor. This highlights the different inhibition modes and/or geometries of the inhibitors and suggests the use of combination or

sequential drug therapies combined with sensitive diagnostics for the appearance of drug resistant strains. We addressed these features in the context of crystal structure information relevant to FLT3 and these drugs.

FLT3 mutations and PDGFR family tyrosine kinase structures. Kinase crystal structures available from the Protein Data Bank[3] that are most closely related to FLT3 include the catalytic and juxtamembrane domains of FLT3 (1RJB; ref. 18), c-FMS (2I0V, 2I0Y, 2I1M, 2OGV, 3BEA), and c- Kit (1pkzg; 1T45, 1T46; refs. 22, 23). In addition, numerous other kinase structures are available that show the binding modes of inhibitors identical to or related to those in this study. Superpositions of these structures with the

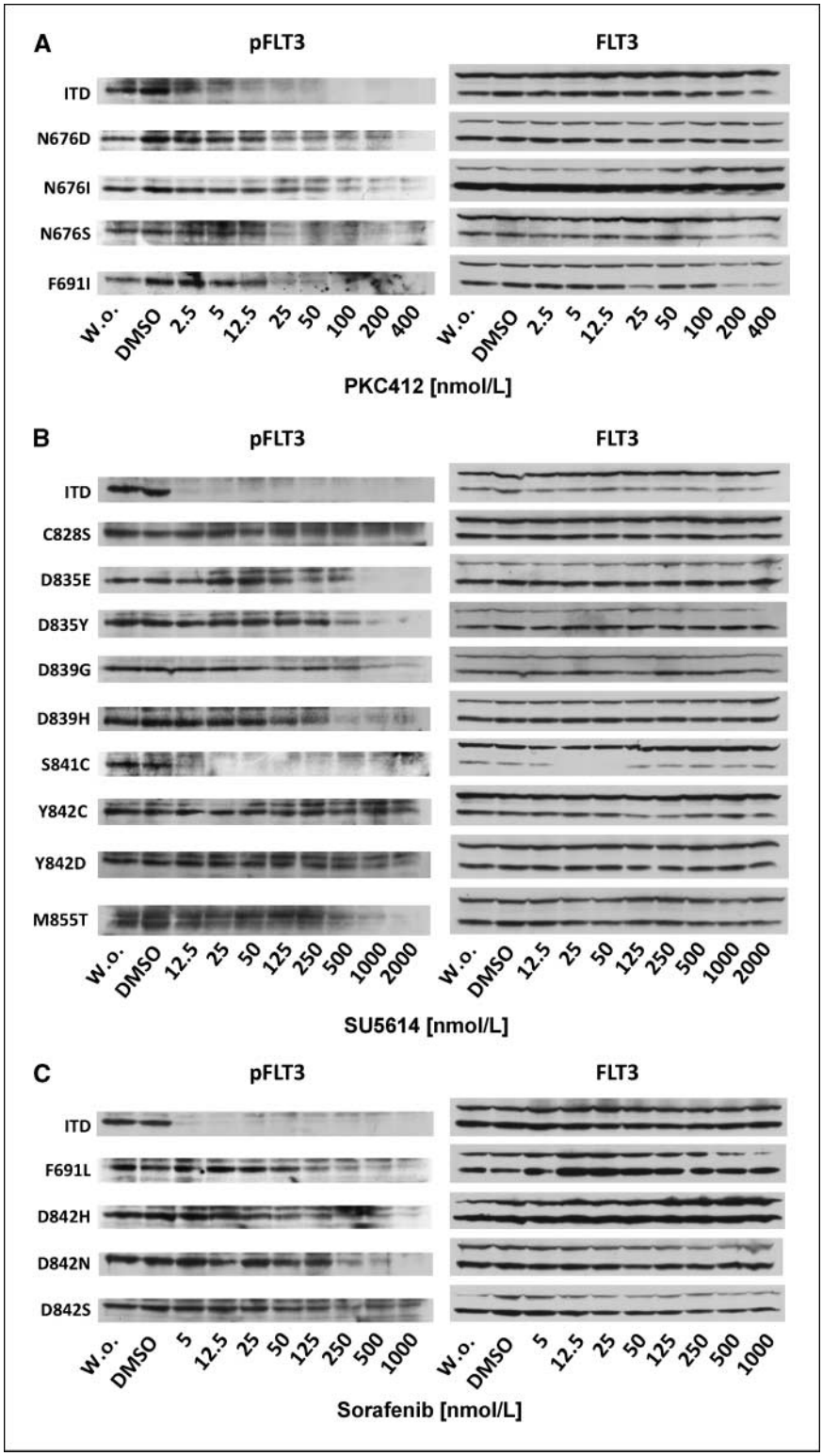

Figure 2. Identified resistance mutations retain FLT3-ITD autophosphorylation in the presence of inhibitor. FLT3-ITD variants identified in resistant clones and FLT3-ITD F691I (21) were cloned. Parental Ba/F3 cells were transformed with wt or mutant constructs. Cells were treated for 2.5 h without and in the presence of PKC412 (*A*), SU5614 (*B*), or sorafenib (*C*) at the indicated concentrations. Whole cell lysates were subjected to SDS-PAGE. Blots were probed for phosphoFLT3 (*left*) and FLT3 (*right*). The FLT3 antibody detected both the mature 155 kDa (cell surface) and the immature 130 kDa (intracellular) form. Due to the presence of the ITD, the phosphoFLT3 antibody mainly detected phosphorylation of the immature form (48).

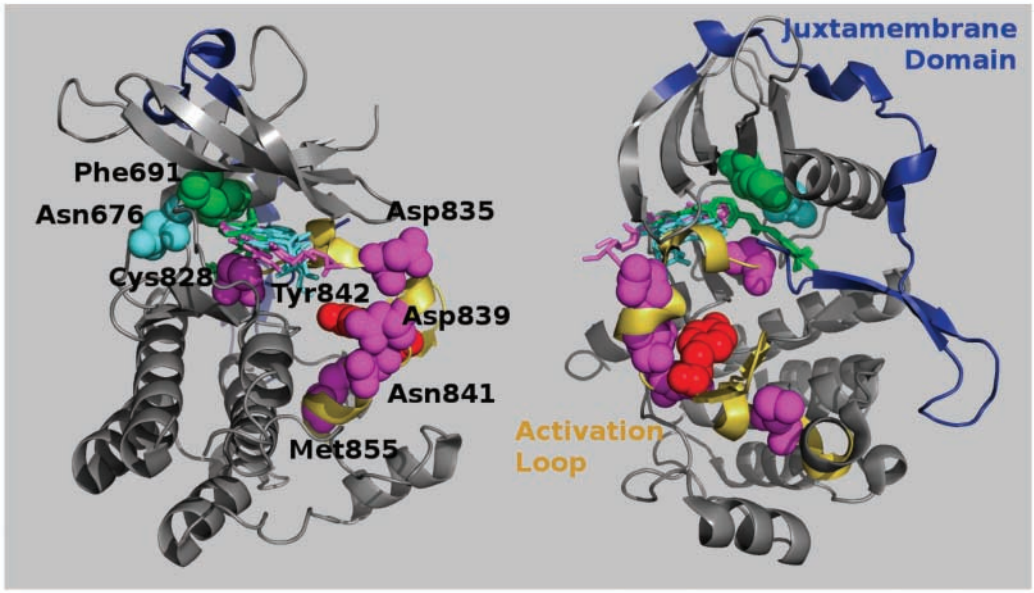

Figure 3. Orthogonal views of the distribution of mutations in FLT3. PKC412 (*cyan sticks*) induced mutations only at a single site N676 (*cyan spheres*). Sorafenib (*green sticks*) induced mutations at the "gatekeeper" F691 (*green spheres*) and the activation loop phosphorylation site Y842 (*red spheres*). SU5614 (*magenta sticks*) induced mutations at Y842 and other sites (*magenta spheres*) in the activation loop. The FLT3 fold is depicted schematically with the activation loop colored yellow and the NH_2-terminal juxtamembrane domain colored blue.

FLT3 structures provide models for FLT3 inhibition by PKC412, sunitinib/SU5614, and sorafenib in FLT3. Many staurosporine and staurosporine derivative structures are available but none of PKC412 (N-benzoyl-staurosporine or midostaurin). The tight binding of PKC412 to FLT3 and correlations of PKC412 and staurosporine binding strengths justify the use of staurosporine structures as a model (24). Two were chosen for this study: 2HZ4 (tetrahydostaurosporine in ABL kinase; ref. 25) and 3D7T (staurosporine in CSK; ref. 26). Sorafenib (BAY 43-9006 or Nexavar) complexes include 1UWH, 1UWJ (wild-type and V599E B-raf, respectively). Sunitinib (SU11248) and SU5614 share a kinase hinge binding scaffold (indolinone), which may be found in the PDB via other cognates as in PDB entry 2JAM. Finally, structure 2z60 provided a kinase domain with an isoleucine residue as a gatekeeper associated with drug resistance.

PKC412 and mutations at N676. The asparagine at position 676 does not likely have direct contacts with any of the inhibitors, so its occurrence may seem surprising. The residue is not highly conserved (less that 65% among tyrosine kinases) outside the PDGFR tyrosine kinase family. However, in the FLT3 structure, the side chain can be seen to structure the loop between the β strands via hydrogen bonds to the main chain, and also with the glutamic acid E692 of the hinge segment (Fig. 4*A*). N676 is highly conserved among the tyrosine kinases that have a single residue glycine insertion at the beginning of the loop, and E692 is also highly conserved. The mutation was observed in a PKC412-resistant patient (10), and was also noted in an *in vitro* mutating PCR screen for resistant mutants, attributed to destabilization of the hinge region (21).

The occurrence of the mutation at this site, not directly in contact with the ATP binding site, together with the low acquired resistance for SU5614 and sorafenib, might indicate that PKC412 binds in a manner different from staurosporine-derived models. Indeed, a partially hydrogenated staurosporine cognate with micromolar IC_{50} activity is seen to bind ABL in alternate locations (pdb code 2HZ4; ref. 25). However, the selectivity patterns for staurosporine and PKC412 are qualitatively similar (24). Furthermore, N659K in PDGFRA, the N676 equivalent position, has been described in GIST (27), and the neighboring V654 in cKit is frequently mutated to alanine in imatinib resistant GIST (see Supplementary Table S1; ref. 28). Taken together, these data support a model for resistance arising from structural effects transmitted to the ATP binding site via an altered loop structure.

The equivalent residue in FGFR2, N549, has been analyzed as one of a triad of residues that form a "molecular brake" (29). This structure contributes to autoinhibition in several tyrosine kinase subfamilies (Supplementary Table S1). Its disruption removes a barrier for rotation of the N-lobe relative to the C-lobe in the formation of an active conformation.

The gatekeeper mutations. With phenylalanine as the gatekeeper residue, FLT3 is unusual among PDGFR family protein kinases. Among the tyrosine kinases, phenylalanine is a typical gatekeeper for Trk receptor kinases, and is otherwise characteristic especially of the CMGC kinases, including, e.g., CDK2 (for which there is a crystal structure of a complex with staurosporine: 1aq1). The relative positions of the inhibitors and F691 are illustrated in Fig. 4*B*. The inhibitors may have aromatic stacking interactions with the gatekeeper. This is especially true for sorafenib, which generated the mutant in these studies. PKC412 may also have stacking interactions, as observed in the CDK2-staurosporine complex structure (pdb entry 1aq1), but the lack of sensitivity to the F691L interaction would show that this type of interaction is not critical to PKC412 binding. In addition, this does not explain the large difference in sensitivities between F691I and F691L variants. Although an isoleucine at the gatekeeper position is commonly observed as a drug resistant mutation, ligand binding

data do not support a hypothesis that the cause is weakened binding to PKC412. For example, the phage display kinase profiling data of Karaman and colleagues (24) shows 10-fold tighter binding of staurosporine for ABL T315I over ABL wt.

The cys mutant. The mutation C828S, generated only by SU5614, leads to moderate resistance for SU5614 and PKC412 but only weak or no resistance for SU11248 and sorafenib. One possible structural explanation for this may be favorable aromat-sulfur interactions.

The superposition of structures places the indolinone of SU5614 directly over the cysteine sulfur with a geometry for which the interaction may contribute significantly to binding energies (30). Similar interactions may play a role in PKC412 binding.

Activation loop mutations. The remaining mutants occur on the activation loop. Modeling the structural determinants of the resistance properties is complicated by the fact that tyrosine kinase activation loops typically display a wide range of structures, variously associated with different states of activity (Fig. 4*C*). The FLT3 crystal structure 1RJB shows the native (and not a oncogenic) protein in an autoinhibited conformation. Thus, consideration of drug effects on secondary mutations of ITD-transformed FLT3 requires the use of a wide variety of indirect structural evidence. The key data that beg explanation include the following: (*a*) Mutation of the phosphorylation site Y842 confers the strongest resistance against SU5614 and sorafenib but little or no resistance against PKC412. Paradoxically, SU5614 does not generate some of the mutants that confer strongest resistance. (*b*) Sorafenib resistance is associated only with Y842 mutation, whereas a variety of activation loop mutations also confer resistance against SU5614.

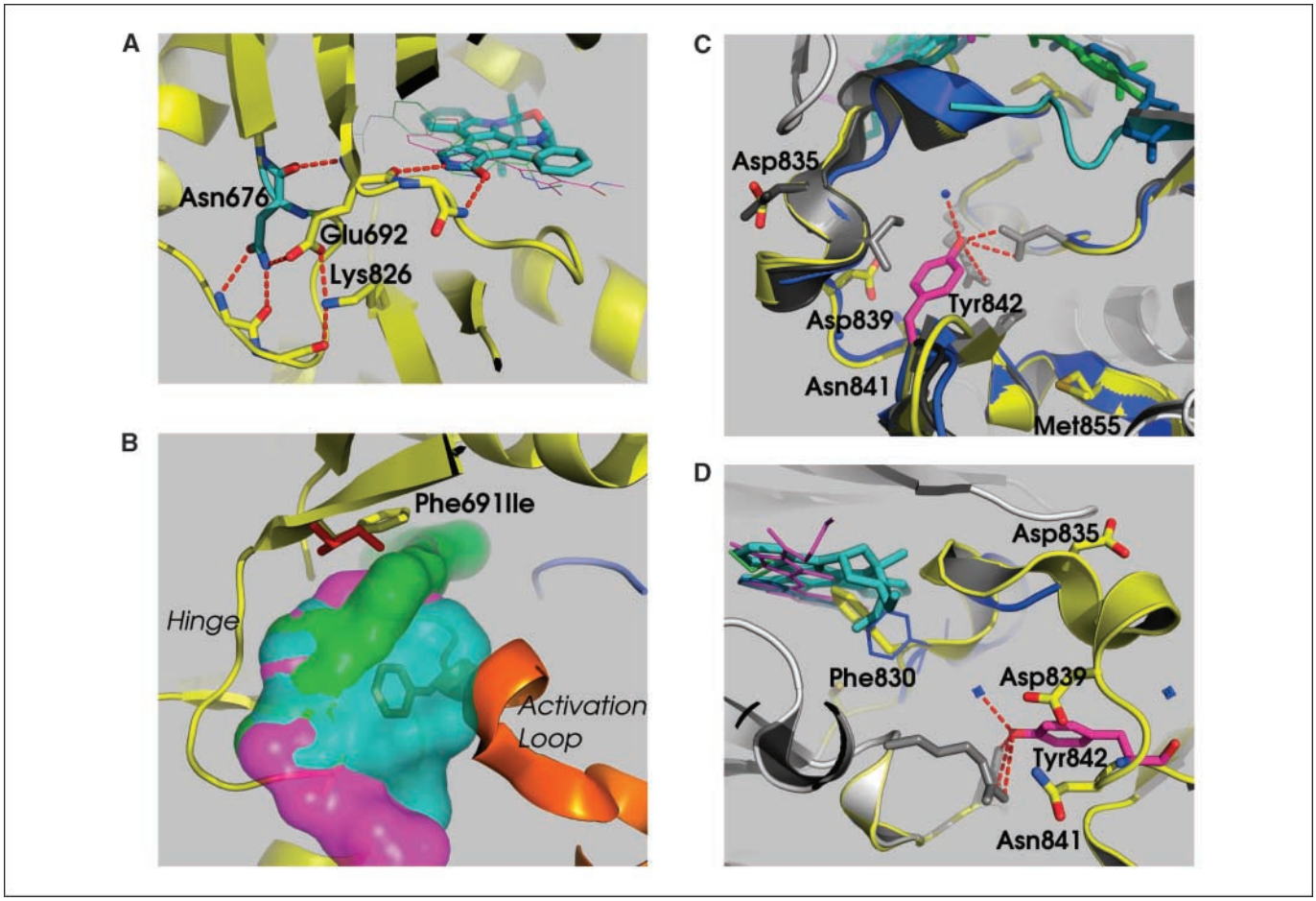

Figure 4. Details of binding at the hinge region (*A* and *B*) and the activation loop (*C* and *D*). Staurosporine (as model for PKC412) is represented as cyan sticks or surface; several superimposed binding positions are shown for the indolinone model for SU5614 (*magenta*) and for sorafenib (*green*). *A,* the role of Asn676 in stabilizing the hinge region is shown by highlighting hydrogen bonding interactions (*red dashes*) between main chain atoms of the residue to the hinge, from the side chain to main chain atoms in the loop, and from the side chain to the conserved glutamic acid at position 692 of the hinge sequence. *B,* inhibitor binding geometries relative to the site of the gatekeeper residue. Superposition of the FLT3 structure (PDB 1RJB; *yellow*) with the structure of the T315I ABL mutant (PDB 2Z60) shows a potential rotamer configuration for the mutant gatekeeper side chain in FLT3 (*red sticks*). Aromatic stacking interactions between the inhibitor and the gatekeeper may be important for inhibitor binding, especially for sorafenib (*green surface*). As with ABL and many PDGFR family tyrosine kinases, the gatekeeper induces strong drug resistance when mutated to isoleucine but not leucine. The steric clash between Phe830 of the activation loop (*B, orange sticks*; *D, blue sticks*) and staurosporine binding is evident. *C* and *D,* alternate views of the activation loop in comparison with c-Kit structures. Superposition of autoinactivated FLT3 (PDB 1RJB) with cKit structures (inactive form, PDB 1T45; imatinib-bound inactive form, PDB 1T46) illustrates the key role of Tyr842 (*violet sticks*) in stabilizing the inactive activating loop fold. Its side chain is buried, forming hydrophobic contacts as well as anchoring polar contacts (*red dashes*). The activation loop folds of FLT3 (*gray cartoon*) autoinhibited by the juxtamembrane domain (*cyan cartoon*) superimposes almost exactly with inactive cKit (*yellow cartoon*). Imatinib-bound cKit (*blue cartoon*) shows a slightly altered inactive conformation. Superposition of the modeled inhibitor geometries shows the similarities between imatinib (*blue sticks*) and sorafenib (*green sticks*; *C*). Although a small shift of the activation loop can resolve the steric clash between imatinib (*blue sticks*) and the Phe of the DFG motif (Phe830 in FLT3, *blue sticks* in *D, orange sticks* in *B*), the clash between PKC412 (here staurosporine; *cyan sticks/spheres*) cannot be relaxed in the same manner (*B* and *D*). By contrast, the modeled positions of SU5614 (*violet sticks/surface*) and sorafenib (*green sticks/surface*) show little or no clash with the activation loop in the inactive geometry.

Although they all bind at the ATP site (see discussion above for possible exceptions), the three inhibitors bind in qualitatively different ways. Figures 3 and 4*C* illustrate how sorafenib binds to the inactive kinase in the inhibitor "type II" mode. Type II inhibitors, including sorafenib, imatinib, and others, occupy a volume (in Fig. 3, *right*, the right half of sorafenib) that is inaccessible when the kinase has a catalytically active geometry. Figure 4*B* and *D* highlight a unique feature of PKC412 binding. Both sorafenib and SU5614 can fit into the autoinhibited FLT3 structure, with only minor adjustments of the activation loop. PKC412 on the other hand would require a large-scale translation of the activation loop main chain to bind. Because FLT3 adopts a range of structures, these qualitative differences seem likely to be related to the qualitatively different patterns of resistance mutations.

The autoinactivation mechanism of FLT3 via juxtamembrane domain binding was shown by the crystal structure 1RJB (18), and is also shown in closely related cKit (23). The internal tandem duplication mutations are thought to activate FLT3 by disrupting the inactivation mechanism (18). Mutations at the activation loop are known to confer constitutive activity to FLT3, presumably by "destabilizing the activation loop" in its autoinhibitor role (e.g., N841I, Y; ref. 31). The observation that many activation loop mutations are able to confer resistance to SU5614 may indicate that this inhibitor partially stabilizes the inactive kinase but becomes ineffective with additional active loop destabilization. In contrast, sorafenib, as a type II inhibitor, can bind to the inactive form and stabilize it more strongly, analogous to imatinib binding of c-Kit (23). Only a small set of activation loop mutations are sufficiently destabilizing the inactive form to render sorafenib ineffective. These involve mutations of Y842 because its interactions most strongly stabilize the inactivated state (Fig. 4*C–D*). PKC412, by contrast, inhibits an active form of the kinase, or at least a form of the kinase in which the activation loop is significantly refolded compared with the inactivated form, and is therefore unaffected by mutations that destabilize the active form.

Discussion

Mutations causing resistance to therapeutic kinase inhibition can be identified in target kinases in various malignant diseases, such as Bcr-Abl in imatinib-resistant chronic myelogenous leukemia (CML; refs. 20, 32), cKit in imatinib-resistant GIST (33), epidermal growth factor receptor in gefitinib-resistant non–small cell lung cancer (34), and FIP1L1-PDGFRA in imatinib-resistant HES/CEL (35). Alternative kinase inhibitors have been developed that can overcome some of the known resistance mutations. The best-studied example is CML, where nilotinib (Tasigna) and dasatinib (Sprycel) showed activity against many of the known imatinib resistance mutations in Bcr-Abl both *in vitro* (36, 37) and in clinical trials (38, 39). Preclinical models have been developed that allow generation of specific resistance profiles in a given drug-target pair (17, 19, 21). Using these strategies, the results for Bcr-Abl and the Abl kinase inhibitors imatinib, nilotinib, and dasatinib show a good correlation of *in vitro* results to clinical findings in patients with CML and resistance to these compounds (17, 40), and predict a narrowed, however largely overlapping, profile of Bcr-Abl resistance mutations for nilotinib and dasatinib compared with imatinib (19, 41, 42).

Here, we show that different ATP competitor–type, small molecule FLT3 inhibitors can produce largely nonoverlapping profiles of secondary resistance mutations in an FLT3-ITD background using a cell-based screening strategy. This finding might reflect distinct binding modes of different inhibitor scaffolds, resulting in distinct conformations of the FLT3 kinase domain available for binding. Screening with SU5614 exclusively produced TK2 exchanges. This is in line with a previous report that identified the FLT3-ITD TK2 mutations Y842H and D835N in SU5614-resistant cell lines (43). All activation loop exchanges retained sensitivity to PKC412, which inhibits an active form of the kinase, and thereby might not be affected by activation loop variants destabilizing the inactive state. In contrast, exchanges emerging in PKC412-resistant clones were limited to position N676 in TK1. Thus far, a single case of a patient with a secondary mutation in FLT3-ITD TK1 (N676K) has been described in the context of PKC412 resistant FLT3-ITD positive AML (10), confirming the clinical significance of this position for PKC412 resistance. Although the N676S exchange was fully responsive to SU5614, the N676I and D exchanges lead to moderate cross-resistance to SU5614. Degenerative PCR-based mutagenesis of FLT3-ITD TK1 and subsequent selection in the presence of PKC412 previously has identified TK1 exchanges causing PKC412 resistance, including two of the three N676 exchanges that we report here (21). In this study, in addition to N676 exchanges, F691I/L and G797R/S were identified. Although FLT3-ITD F691L only slightly interferes with PKC412 response (cellular IC_{50} is 10 nmol/L in our hands), F691I leads to a strong PKC412 resistance and therefore should also come up in a cell-based screen. However, we were able to identify an F691 exchange only in the sorafenib screen, probably because the yield of resistant clones using PKC412 in a cell-based approach is limited by PKC412 toxicity. Pharmacokinetic analyses of PKC412 in phase 1 and 2 clinical trials showed that plasma concentrations in the range of 5 μmol/L can be achieved (8, 44). However, declining concentrations over time and high plasma protein binding can result in actual drug levels in the range of 50 nmol/L or lower (8, 10, 44). Thus, PKC412 at 100 nmol/L, the concentration we selected for screening might very well reflect actual drug levels achievable in treated patients. Although PKC412 at 50 nmol/L still would be sufficient to fully inhibit wild-type FLT3-ITD or secondary TK2 mutations identified with SU5614 and sorafenib in this study, this concentration clearly would not be adequate to suppress N676D, N676I, or F691I.

FLT3-ITD F691I is the only exchange causing strong resistance not only to PKC412 but also to SU5614, SU11248, and sorafenib. Thus, once FLT3-ITD F691I emerges in the clinic, a switch to a different FLT3 inhibitor probably would not be effective. However, the use of the dual PI3K/PDK-1 inhibitor BAG956 (45), combinations of PKC412 and the mammalian target of rapamycin inhibitor, rapamycin (46) or the IAP inhibitor, LBW242 (47), have shown activity against FLT3-ITD F691I in cell lines.

The indolinone SU11248 (Sunitinib, Sutent) and the biaryl urea BAY 43-9006 (Sorafenib, Nexavar) recently entered clinical testing in FLT3 mutated (Sunitinib) and FLT3 wt and mutated AML (Sorafenib; refs. 15, 48). Steady-state plasma levels of up to 1 μmol/L for sunitinib and 4 μmol/L for sorafenib have been reported in phase I trials in solid tumors (49). Interestingly, when we performed cross-resistance studies with both compounds, we noted that TK2 exchanges identified with SU5614 did not cause relevant cross-resistance to SU11248. Furthermore, N676 exchanges generated with PKC412 were fully suppressed at 500 nmol/L SU11248. This was also the case for sorafenib with the exception of Y842D, which shifted cellular IC_{50} 30-fold to 250 nmol/L. In

accordance, screening with sorafenib produced a distinct set of resistance mutations at positions D842(H/N/S) and F691L, and these exchanges resulted in a profound, clinically significant resistance to sorafenib. Although the finding of F691I/L causing strong sorafenib resistance already has been reported (50), it is interesting to note that sorafenib resistance mutations in FLT3-ITD TK2 seem to be restricted to a very specific subset of Y842 exchanges, namely Y842D/H/N and S but not Y842C or exchanges at S841. As noted, this might be because only the key Y842 mutants sufficiently destabilize the inactive form to interfere with sorafenib binding. However, all Y842 exchanges were responsive to PKC412, and at clinically achievable concentrations, also to SU11248.

Taken together, we provide a comprehensive prediction of FLT3-ITD TK1 and TK2 resistance mutations that might develop in the treatment of FLT3-ITD–positive AML with specific FLT3 inhibitors. Our data indicate that unlike the scenario in CML, where different ABL kinase inhibitors display largely overlapping resistance profiles, the pattern of specific resistance mutations is essentially nonoverlapping for different FLT3 kinase inhibitors. This not only contributes important information for sequential treatment strategies in FLT3-ITD–positive AML but also constitutes a strong rational for primary combinations of FLT3 kinase inhibitors with nonoverlapping resistance patterns, alone or in combination with chemotherapy in a genetically highly instable disease.

Disclosure of Potential Conflicts of Interest

N. von Bubnoff and J. Duyster served as advisors for Novartis. The other authors disclosed no potential conflicts of interest.

Acknowledgments

Received 7/30/08; revised 12/11/08; accepted 1/19/09; published OnlineFirst 3/24/09.

Grant support: The José Carreras Stiftung No. 106682 and by a grant from the Bundesministerium für Bildung und Forchung (NGFNplus; J. Duyster and N. von Bubnoff). J. Duyster is supported by a grant from the Mildred-Scheel Stiftung (Oncogene networks in AML) and SFB 684 from the Deutschefs Forschungsgemeinschaft.

The costs of publication of this article were defrayed in part by the payment of page charges. This article must therefore be hereby marked *advertisement* in accordance with 18 U.S.C. Section 1734 solely to indicate this fact.

References

1. Birg F, Courcoul M, Rosnet O, et al. Expression of the FMS/KIT-like gene FLT3 in human acute leukemias of the myeloid and lymphoid lineages. Blood 1992;80:2584–93.
2. Levis M, Small D. FLT3: ITDoes matter in leukemia. Leukemia 2003;17:1738–52.
3. Thiede C, Steudel C, Mohr B, et al. Analysis of FLT3-activating mutations in 979 patients with acute myelogenous leukemia: association with FAB subtypes and identification of subgroups with poor prognosis. Blood 2002;99:4326–35.
4. Mizuki M, Fenski R, Halfter H, et al. Flt3 mutations from patients with acute myeloid leukemia induce transformation of 32D cells mediated by the Ras and STAT5 pathways. Blood 2000;96:3907–14.
5. Kelly LM, Liu Q, Kutok JL, Williams IR, Boulton CL, Gilliland DG. FLT3 internal tandem duplication mutations associated with human acute myeloid leukemias induce myeloproliferative disease in a murine bone marrow transplant model. Blood 2002;99:310–8.
6. Weisberg E, Boulton C, Kelly LM, et al. Inhibition of mutant FLT3 receptors in leukemia cells by the small molecule tyrosine kinase inhibitor PKC412. Cancer Cell 2002;1:433–43.
7. Levis M, Allebach J, Tse KF, et al. A FLT3-targeted tyrosine kinase inhibitor is cytotoxic to leukemia cells *in vitro* and *in vivo*. Blood 2002;99:3885–91.
8. Stone RM, DeAngelo DJ, Klimek V, et al. Patients with acute myeloid leukemia and an activating mutation in FLT3 respond to a small-molecule FLT3 tyrosine kinase inhibitor, PKC412. Blood 2005;105:54–60.
9. Knapper S, Burnett AK, Littlewood T, et al. A phase 2 trial of the FLT3 inhibitor lestaurtinib (CEP701) as first-line treatment for older patients with acute myeloid leukemia not considered fit for intensive chemotherapy. Blood 2006;108:3262–70.
10. Heidel F, Solem FK, Breitenbuecher F, et al. Clinical resistance to the kinase inhibitor PKC412 in acute myeloid leukemia by mutation of Asn-676 in the FLT3 tyrosine kinase domain. Blood 2006;107:293–300.
11. Knapper S. FLT3 inhibition in acute myeloid leukaemia. Br J Haematol 2007;138:687–99.
12. Fiedler W, Serve H, Dohner H, et al. A phase 1 study of SU11248 in the treatment of patients with refractory or resistant acute myeloid leukemia (AML) or not amenable to conventional therapy for the disease. Blood 2005;105:986–93.
13. Auclair D, Miller D, Yatsula V, et al. Antitumor activity of sorafenib in FLT3-driven leukemic cells. Leukemia 2007;21:439–45.
14. Kancha RK, Grundler R, Peschel C, Duyster J. Sensitivity toward sorafenib and sunitinib varies between different activating and drug-resistant FLT3-ITD mutations. Exp Hematol 2007;35:1522–6.
15. Zhang W, Konopleva M, Shi YX, et al. Mutant FLT3: a direct target of sorafenib in acute myelogenous leukemia. J Natl Cancer Inst 2008;100:184–98.
16. Grundler R, Thiede C, Miething C, Steudel C, Peschel C, Duyster J. Sensitivity toward tyrosine kinase inhibitors varies between different activating mutations of the FLT3 receptor. Blood 2003;102:646–51.
17. von Bubnoff N, Veach DR, van der Kuip H, et al. A cell-based screen for resistance of Bcr-Abl-positive leukemia identifies the mutation pattern for PD166326, an alternative Abl kinase inhibitor. Blood 2005;105:1652–9.
18. Griffith J, Black J, Faerman C, et al. The structural basis for autoinhibition of FLT3 by the juxtamembrane domain. Mol Cell 2004;13:169–78.
19. Bradeen HA, Eide CA, O'Hare T, et al. Comparison of imatinib mesylate, dasatinib (BMS-354825), and nilotinib (AMN107) in an N-ethyl-N-nitrosourea (ENU)-based mutagenesis screen: high efficacy of drug combinations. Blood 2006;108:2332–8.
20. Gorre ME, Mohammed M, Ellwood K, et al. Clinical resistance to STI-571 cancer therapy caused by BCR-ABL gene mutation or amplification. Science 2001;293:876–80.
21. Cools J, Mentens N, Furet P, et al. Prediction of resistance to small molecule FLT3 inhibitors: implications for molecularly targeted therapy of acute leukemia. Cancer Res 2004;64:6385–9.
22. Mol CD, Lim KB, Sridhar V, et al. Structure of a c-kit product complex reveals the basis for kinase transactivation. J Biol Chem 2003;278:31461–4.
23. Mol CD, Dougan DR, Schneider TR, et al. Structural basis for the autoinhibition and STI-571 inhibition of c-Kit tyrosine kinase. J Biol Chem 2004;279:31655–63.
24. Karaman MW, Herrgard S, Treiber DK, et al. A quantitative analysis of kinase inhibitor selectivity. Nat Biotechnol 2008;26:127–32.
25. Cowan-Jacob SW, Fendrich G, Floersheimer A, et al. Structural biology contributions to the discovery of drugs to treat chronic myelogenous leukaemia. Acta Crystallogr D Biol Crystallogr 2007;63:80–93.
26. Levinson NM, Seeliger MA, Cole PA, Kuriyan J. Structural basis for the recognition of c-Src by its inactivator Csk. Cell 2008;134:124–34.
27. Corless CL, Schroeder A, Griffith D, et al. PDGFRA mutations in gastrointestinal stromal tumors: frequency, spectrum and *in vitro* sensitivity to imatinib. J Clin Oncol 2005;23:5357–64.
28. Heinrich MC, Corless CL, Blanke CD, et al. Molecular correlates of imatinib resistance in gastrointestinal stromal tumors. J Clin Oncol 2006;24:4764–74.
29. Chen H, Ma J, Li W, et al. A molecular brake in the kinase hinge region regulates the activity of receptor tyrosine kinases. Mol Cell 2007;27:717–30.
30. Meyer EA, Castellano RK, Diederich F. Interactions with aromatic rings in chemical and biological recognition. Angew Chem Int Ed Engl 2003;42:1210–50.
31. Jiang J, Paez JG, Lee JC, et al. Identifying and characterizing a novel activating mutation of the FLT3 tyrosine kinase in AML. Blood 2004;104:1855–8.
32. von Bubnoff N, Schneller F, Peschel C, Duyster J. BCR-ABL gene mutations in relation to clinical resistance of Philadelphia-chromosome-positive leukaemia to STI571: a prospective study. Lancet 2002;359:487–91.
33. Tamborini E, Bonadiman L, Greco A, et al. A new mutation in the KIT ATP pocket causes acquired resistance to imatinib in a gastrointestinal stromal tumor patient. Gastroenterology 2004;127:294–9.
34. Kobayashi S, Boggon TJ, Dayaram T, et al. EGFR mutation and resistance of non-small-cell lung cancer to gefitinib. N Engl J Med 2005;352:786–92.
35. Cools J, DeAngelo DJ, Gotlib J, et al. A tyrosine kinase created by fusion of the PDGFRA and FIP1L1 genes as a therapeutic target of imatinib in idiopathic hypereosinophilic syndrome. N Engl J Med 2003;348:1201–14.
36. Weisberg E, Manley PW, Breitenstein W, et al. Characterization of AMN107, a selective inhibitor of native and mutant Bcr-Abl. Cancer Cell 2005;7:129–41.
37. Shah NP, Tran C, Lee FY, Chen P, Norris D, Sawyers CL. Overriding imatinib resistance with a novel ABL kinase inhibitor. Science 2004;305:399–401.
38. Guilhot F, Apperley J, Kim DW, et al. Efficacy of Dasatinib in Patients with Accelerated-Phase Chronic Myelogenous Leukemia with Resistance or Intolerance to Imatinib: 2-Year Follow-Up Data from START-A (CA180–005). 49th ASH Annual Meeting; 2007; Atlanta: Blood; 2007. p. 145A.
39. Saglio G, Kim DW, Hochhaus A, et al. Correlation of Clinical Response to Nilotinib with BCR-ABL Mutation Status in Advanced Phase Chronic Myelogenous Leukemia (CML-AP) Patients with Imatinib-Resistance or Intolerance. 49th ASH Annual Meeting; 2007; Atlanta: Blood; 2007. p. 576–7A.
40. Cortes J, Jabbour E, Kantarjian H, et al. Dynamics of BCR-ABL kinase domain mutations in chronic myeloid leukemia after sequential treatment with multiple tyrosine kinase inhibitors. Blood 2007;110:4005–11.
41. Burgess MR, Skaggs BJ, Shah NP, Lee FY, Sawyers CL. Comparative analysis of two clinically active BCR-ABL kinase inhibitors reveals the role of conformation-specific

binding in resistance. Proc Natl Acad Sci U S A 2005;102:3395–400.
42. von Bubnoff N, Manley PW, Mestan J, Sanger J, Peschel C, Duyster J. Bcr-Abl resistance screening predicts a limited spectrum of point mutations to be associated with clinical resistance to the Abl kinase inhibitor nilotinib (AMN107). Blood 2006;108:1328–33.
43. Bagrintseva K, Schwab R, Kohl TM, et al. Mutations in the tyrosine kinase domain of FLT3 define a new molecular mechanism of acquired drug resistance to PTK inhibitors in FLT3-ITD-transformed hematopoietic cells. Blood 2004;103:2266–75.
44. Propper DJ, McDonald AC, Man A, et al. Phase I and pharmacokinetic study of PKC412, an inhibitor of protein kinase C. J Clin Oncol 2001;19:1485–92.
45. Weisberg E, Banerji L, Wright RD, et al. Potentiation of antileukemic therapies by the dual PI3K/PDK-1 inhibitor, BAG956: effects on BCR-ABL- and mutant FLT3-expressing cells. Blood 2008;111:3723–34.
46. Mohi MG, Boulton C, Gu TL, et al. Combination of rapamycin and protein tyrosine kinase (PTK) inhibitors for the treatment of leukemias caused by oncogenic PTKs. Proc Natl Acad Sci U S A 2004;101:3130–5.
47. Weisberg E, Kung AL, Wright RD, et al. Potentiation of antileukemic therapies by Smac mimetic, LBW242: effects on mutant FLT3-expressing cells. Mol Cancer Ther 2007;6:1951–61.
48. O'Farrell AM, Foran JM, Fiedler W, et al. An innovative phase I clinical study demonstrates inhibition of FLT3 phosphorylation by SU11248 in acute myeloid leukemia patients. Clin Cancer Res 2003;9:5465–76.
49. Strumberg D, Richly H, Hilger RA, et al. Phase I clinical and pharmacokinetic study of the Novel Raf kinase and vascular endothelial growth factor receptor inhibitor BAY 43–9006 in patients with advanced refractory solid tumors. J Clin Oncol 2005;23:965–72.
50. Lierman E, Lahortiga I, Van Miegroet H, Mentens N, Marynen P, Cools J. The ability of sorafenib to inhibit oncogenic PDGFRβ and FLT3 mutants and overcome resistance to other small molecule inhibitors. Haematologica 2007;92:27–34.